

# Facile synthesis of ordered mesoporous carbons from F108/resorcinol–formaldehyde composites obtained in basic media

Changyi Liu, Lixia Li, Huaihe Song\* and Xiaohong Chen

Received (in Cambridge, UK) 29th September 2006, Accepted 31st October 2006

First published as an Advance Article on the web 19th December 2006

DOI: 10.1039/b614199d

**Highly ordered mesoporous carbon with cubic  $Im\bar{3}m$  symmetry has been synthesized successfully via a direct carbonization of self-assembled F108 (EO<sub>132</sub>PO<sub>50</sub>EO<sub>132</sub>) and resorcinol–formaldehyde (RF) composites obtained in a basic medium of nonaqueous solution.**

Ordered mesoporous carbon materials have been attracting considerable attention because of their potential applications<sup>1–3</sup> in gas separation, catalyst supports, and energy storage/conversion. They have been mainly fabricated by employing ordered mesoporous silicas as hard templates during the past few years, which generally involved pre-synthesis of ordered mesoporous silicas, repeated impregnation with carbon precursors, drying, carbonization and subsequent removal of the hard templates by NaOH or HF solution.<sup>4–8</sup> Obviously, this is a time-consuming and high-cost procedure. Although it was once simplified,<sup>9</sup> the use of hard templates is still unavoidable. More recently, several research groups<sup>10–15</sup> have developed some simple routes for the synthesis of ordered mesoporous carbons directly derived from organic–organic composites by self-assembly of block copolymers. For example, Dai *et al.*<sup>10</sup> prepared well-ordered mesoporous carbons via a stepwise assembly approach. The resorcinol monomers were pre-organized into a well-ordered nanostructured film by self-assembly of polystyrene-*block*-poly(4-vinylpyridine) (PS-*P4VP*), followed by the *in situ* polymerization of resorcinol and formaldehyde vapor to form resorcinol–formaldehyde resin (RFR). Zhao *et al.*<sup>11,15</sup> synthesized ordered mesoporous polymers and carbon frameworks using resol (phenol–formaldehyde) as a carbon precursor and a triblock copolymer as a template via a solvent evaporation induced self-assembly method (EISA). Ordered mesoporous materials with different structures, such as 2D hexagonal ( $p6m$ ), 3D caged cubic ( $Im\bar{3}m$ ) and lamellar frameworks, can be obtained by adjusting the mass ratio of the carbon precursor and triblock copolymer. Tanaka *et al.*<sup>12</sup> reported the synthesis of ordered mesoporous carbons with a hexagonal channel structure by a direct carbonization of organic–organic composites prepared using RF and triethyl orthoacetate (EOA) as the carbon co-precursors in strongly acidic media. Here EOA plays a crucial role in the stabilization of the ordered mesostructure.

It is well known that under acidic conditions RF forms mainly linear polymeric chains or polymeric networks with a low degree of cross-linking,<sup>16</sup> and thus the frameworks of organic–organic composites obtained by self-assembly of block copolymers easily

collapse during carbonization. However, polymeric networks with a high degree of cross-linking can be obtained under basic conditions. Herein, we report the direct synthesis of highly ordered mesoporous carbons with a cubic structure of  $Im\bar{3}m$  symmetry in a basic medium of nonaqueous solution. Pluronic F108 (triblock poly(ethylene oxide)–poly(propylene oxide)–poly(ethylene oxide), EO<sub>132</sub>PO<sub>50</sub>EO<sub>132</sub>, MW = 14 600, Sigma-Aldrich) was used as a structure-directing agent and RF sol as a carbon precursor. The essence of the synthesis is to first form a periodic mesostructure through the hydrogen bonding interaction between RF sol, with many hydroxyl groups (–OH), and F108. Upon pyrolysis, the porous carbon structures are directly generated with the decomposition of the structure-directing agent.

In a typical synthesis, firstly, 2.0 g of F108 was dissolved in 15.0 g of ethanol under magnetic stirring at 30 °C. Then, the RF sol was synthesized as follows: 2.0 g of resorcinol and 0.050 g of solid NaOH were together dissolved in 30.0 g of ethanol, followed by addition of 4.4 g of 37% formaldehyde and stirring at room temperature until the solution became light yellow. Subsequently, the RF sol was divided into two equal parts: one part was cured at 100 °C for 24 h to form the RFR, after the complete evaporation of ethanol. The other part was added dropwise to the above ethanol solution containing F108, further stirred for 1 h until the colour turned light red, and then was poured into a glass dish. A glue-like film was formed by the evaporation of ethanol, and then was cured at 100 °C for 24 h in air to generate the F108/RF composite. Finally, the composite was carbonized at 400 or 700 °C for 3 h, with a heating rate of 1 °C min<sup>–1</sup> under a nitrogen atmosphere, to obtain the ordered mesoporous carbons (herein-after, the two carbon samples are abbreviated as C-400 and C-700, respectively).

X-Ray diffraction (XRD) patterns of the as-synthesized and carbonized samples are shown in Fig. 1. The as-synthesized F108/RF composite shows a well-resolved diffraction peak at  $2\theta = 0.67^\circ$ . With the heat-treatment in a nitrogen gas atmosphere, the diffraction peak is shifted to a higher angle, *i.e.*,  $2\theta = 0.85^\circ$  for C-400 and  $0.96^\circ$  for C-700, due to the structural shrinkage resulting from carbonization. For C-400, the XRD pattern is more resolved, and four additional weak diffraction peaks can be clearly observed in the region of  $2\theta = 1–2^\circ$  (see Fig. 1 inset). Combined with transmission electron microscope (TEM) analysis (see Fig. 2), these diffraction peaks can be indexed to (110), (200), (211), (220), and (310) reflections of the ordered body-centered cubic structure with  $Im\bar{3}m$  space group.<sup>17</sup> The cell parameters ( $a$ ) are calculated to be 18.5, 14.7, and 13.0 nm for the as-synthesized composite, C-400 and C-700, respectively. Apparently, the high-temperature process gives rise to relatively large shrinkage in the cell parameter ( $ca$

State Key Laboratory of Chemical Resource Engineering, Beijing University of Chemical Technology, Beijing, 10029, P. R. China.  
E-mail: songhh@mail.buct.edu.cn (H.Song); Fax: +86 10 64434916;  
Tel: +86 10 64434916

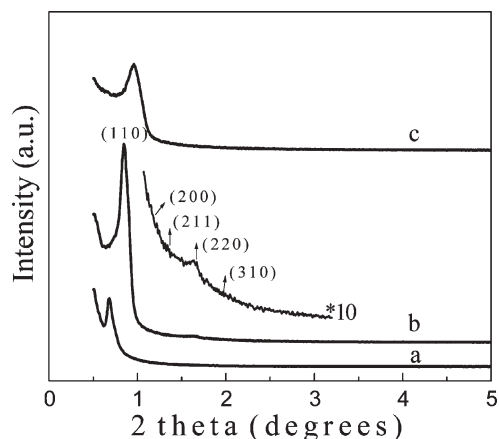


**Fig. 1** Powder XRD patterns of (a) as-synthesized F108/RF composite, (b) C-400 (inset: C-400  $2\theta = 1\text{--}3^\circ$  at 10x magnification) and (c) C-700. XRD patterns were recorded on a Rigaku D/max-2500B2+/PCX system operating at 40 kV and 20 mA using  $\text{CuK}\alpha$  radiation ( $\lambda = 1.5406 \text{ \AA}$ ).

20 and 30% for C-400 and C-700, respectively). In addition, the (110) diffraction peak of C-700 becomes broader in comparison with that of the as-synthesized composite and C-400, and the other four weak diffraction peaks are hardly discernible. These changes may result from the partial collapse of the ordered mesostructure during the higher temperature treatment. Even so, the structural order was still retained, as shown in Fig. 2d.

High-resolution transmission electron microscope (HRTEM) images of C-400 are shown in Fig. 2. The mesostructure arrangements with long-range order are visible along the [111],

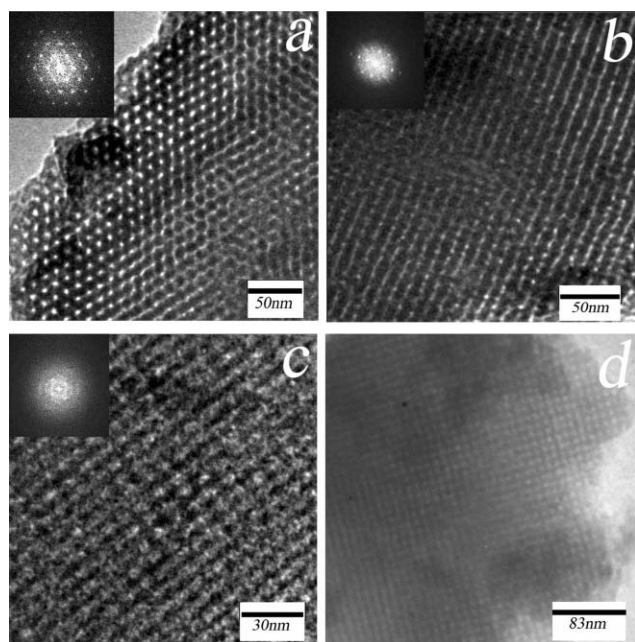


**Fig. 2** HRTEM images of C-400: (a) along the [111] direction, (b) along the [110] direction and (c) along the [100] direction; (d) TEM image of C-700. The corresponding Fourier diffractograms are inset in each image. HRTEM images were recorded on a JEM-3010 microscope operating at an accelerating voltage of 300 kV. The TEM micrograph was obtained using a Hitachi H-800 transmission electron microscope operating at 200 kV.

[110], and [100] directions. Combined with the corresponding Fourier diffractograms, the ordered cubic ( $Im\bar{3}m$ ) mesostructure is further confirmed from these images. C-700 has the similar mesostructure as well, indicating that the ordered mesostructure is thermally stable. The cell parameter of C-400 estimated from the images is approximately 15.0 nm, in good agreement with the value determined from the XRD data. The corresponding pore size of this sample is estimated to be about 7.0 nm, which is consistent with the following nitrogen adsorption–desorption analysis.

Nitrogen adsorption–desorption isotherms and BJH pore size distributions for the carbonized samples are presented in Fig. 3. It can be clearly seen that the isotherms show type-IV curves, reflecting the characteristics of mesoporous materials, regardless of the carbonization temperature. The appearance of  $\text{H}_2$ -type hysteresis loops in the isotherms indicates a 3D cage-like pore structure.<sup>18</sup> C-400 and C-700 have pore size distributions centered at 6.3 and 4.9 nm, respectively, suggesting that the samples have uniform pore structures. In contrast to C-400, C-700 possesses a broader pore size distribution, which may arise from the strong cracking of RFR during high-temperature carbonization. Thus, the ordered mesostructure was partially destroyed as a result of the collapse of some pore walls, which can also be evidenced from the isotherm of C-700. The BET surface areas of C-400 and C-700 are 413 and 564  $\text{m}^2 \text{ g}^{-1}$  and the corresponding pore volumes are 0.39 and 0.25  $\text{cm}^3 \text{ g}^{-1}$ , respectively.

Fig. 4 shows thermogravimetric (TG) and derivative thermogravimetric (DTG) curves of three samples: RFR, F108 and F108/RF composite. The TG curve of the RFR exhibits a continuous weight loss from 200 to 750  $^\circ\text{C}$ . The F108 starts to decompose at 290  $^\circ\text{C}$  and finishes at 400  $^\circ\text{C}$  with only negligible residue (3.5 wt%). A significant weight loss of about 60% occurs from 250 to 400  $^\circ\text{C}$  for the F108/RF composite, which is mainly attributed to the decomposition of F108. Therefore, it is reasonable to choose  $T = 400 \text{ }^\circ\text{C}$  as a proper pyrolysis temperature for preparing ordered mesoporous carbon, because most of the block copolymers have been degraded at this temperature, whereas the weight of the RFR has not exhibited a significant decrease. In addition, compared with F108, F108/RF composite possesses the higher decomposition temperature corresponding to the maximum weight loss from the DTG curves (386 and 375  $^\circ\text{C}$  for F108/RF composite and

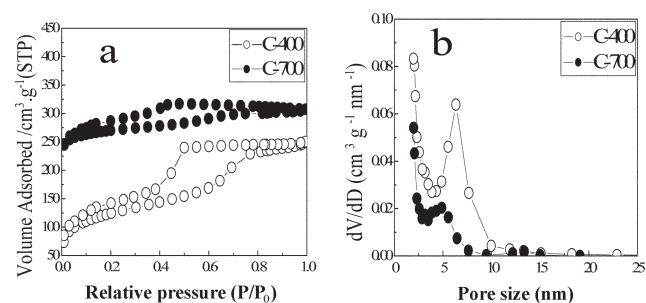


**Fig. 3** (a) Nitrogen adsorption–desorption isotherms and (b) pore size distributions for C-400 and C-700.  $\text{N}_2$  sorption measurements were performed at 77 K on an ASAP 2020 Micromeritics Instrument, all the samples were degassed at 250  $^\circ\text{C}$  overnight on a vacuum line. The pore size distributions were calculated from the adsorption branch of the isotherms by the Barrett–Joyner–Halanda (BJH) model. The isotherm of C-700 is offset vertically by 100  $\text{cm}^3 \text{ g}^{-1}$ .

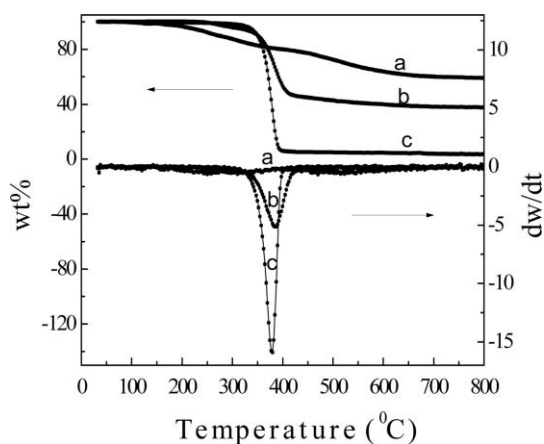


**Fig. 4** Thermogravimetric and derivative thermogravimetric curves for (a) RFR, (b) F108/RF and (c) F108. Thermogravimetric analysis (TGA) was conducted under a flow of argon ( $24 \text{ ml min}^{-1}$ ) at a heating rate of  $5 \text{ }^\circ\text{C min}^{-1}$  from room temperature to  $800 \text{ }^\circ\text{C}$  on a NETZSCH STA449C simultaneous thermal instrument.

F108, respectively), implying that the addition of RF affects the pyrolysis of F108, especially the PEO segments. It was reported that RF is localized in the PEO region of F108,<sup>14,19,20</sup> and can be tangled strongly with PEO chains by the interaction of hydrogen bonding. In particular, the longer PEO blocks in F108 are very beneficial for the formation of more stable hydrogen bonding networks with the polar groups of RF. As a result, the decomposition temperature of F108 may be retarded by RF. Moreover, it is also important to note that a slow heating rate was needed in order to minimize structural deformation of the pores during the removal of the block copolymer.

In the experiment, the hydrogen bonding plays an important role in driving the self-assembly of RF sol and F108 to form periodically ordered composites. Upon further polymerization at  $100 \text{ }^\circ\text{C}$ , the highly cross-linked polymeric networks are formed, which are responsible for the final ordered mesostructure after the higher temperature pyrolysis. Furthermore, the F108/resorcinol (F108/R) mass ratio is also a decisive factor for the resultant mesostructure. It was found that the ordered mesostructure cannot be obtained when the F108/R mass ratio is lower than 1.0 or higher than 3.0. When the F108/R mass ratio is lower than 1.0, it is difficult to form lyotropic liquid crystals in the less concentrated F108 solution. However, much thinner pore walls are probably formed when the F108/R mass ratio is higher than 3.0, which are unfavorable for the further carbonization at higher temperature.

In summary, highly ordered mesoporous carbon with a cage-like structure has been directly synthesized by utilizing F108 as a structure-directing agent and RF sol as a carbon precursor in a basic medium of nonaqueous solution *via* an evaporation induced self-assembly method. We expect to synthesize ordered mesoporous carbons with a variety of mesostructures by choosing appropriate structure-directing agents and optimizing the synthetic parameters. This simple and effective approach would promote the applications in many fields.

This work was supported by the Research Program of China Petrochemical Corporation (X504014) and the Program for New Century Excellent Talents in University of China (NCET-04-0122).

## Notes and references

- 1 S. H. Joo, S. J. Choi, I. Oh, J. Kwak, Z. Liu, O. Terasaki and R. Ryoo, *Nature*, 2001, **412**, 169.
- 2 A. C. Dillon, K. M. Jones, T. A. Bekkedahl, C. H. Kiang, D. S. Bethune and M. J. Heben, *Nature*, 1997, **386**, 377.
- 3 J. Lee, S. Yoon, T. Hyeon, S. M. Oh and K. B. Kim, *Chem. Commun.*, 1999, 2177.
- 4 R. Ryoo, S. H. Joo and S. Jun, *J. Phys. Chem. B*, 1999, **103**, 7743.
- 5 S. Jun, S. H. Joo, R. Ryoo, M. Kruk, M. Jaroniec, Z. Liu, T. Ohsuna and O. Terasaki, *J. Am. Chem. Soc.*, 2000, **122**, 10712.
- 6 R. Ryoo, S. H. Joo, M. Kruk and M. Jaroniec, *Adv. Mater.*, 2001, **13**, 677.
- 7 B. Tian, S. Che, Z. Liu, X. Liu, W. Fan, T. Tatsumi, O. Terasaki and D. Zhao, *Chem. Commun.*, 2003, 2726.
- 8 Y. Sakamoto, T. W. Kim, R. Ryoo and O. Terasaki, *Angew. Chem., Int. Ed.*, 2004, **43**, 5231.
- 9 L. Li, H. Song and X. Chen, *Microporous Mesoporous Mater.*, 2006, **94**, 9.
- 10 C. Liang, K. Hong, G. A. Guiochon, J. W. Mays and S. Dai, *Angew. Chem., Int. Ed.*, 2004, **43**, 5785.
- 11 Y. Meng, D. Gu, F. Zhang, Y. Shi, H. Yang, Z. Li, C. Yu, B. Tu and D. Zhao, *Angew. Chem., Int. Ed.*, 2005, **44**, 7053.
- 12 S. Tanaka, N. Nishiyama, Y. Egashira and K. Ueyama, *Chem. Commun.*, 2005, 2125.
- 13 F. Zhang, Y. Meng, D. Gu, Y. Yan, C. Yu, B. Tu and D. Zhao, *J. Am. Chem. Soc.*, 2005, **127**, 13508.
- 14 C. Liang and S. Dai, *J. Am. Chem. Soc.*, 2006, **128**, 5316.
- 15 Y. Meng, D. Gu, F. Zhang, Y. Shi, L. Cheng, D. Feng, Z. Wu, Z. Chen, Y. Wan, A. Stein and D. Zhao, *Chem. Mater.*, 2006, **18**, 4447.
- 16 A. Knop and L. A. Pilato, *Phenolic Resins—Chemistry, Applications and Performance, Future Directions*, Springer, Berlin, 1985.
- 17 D. Zhao, Q. Huo, J. Feng, B. F. Chmelka and G. D. Stucky, *J. Am. Chem. Soc.*, 1998, **120**, 6024.
- 18 J. R. Matos, M. Kruk, L. P. Mercuri, M. Jaroniec, L. Zhao, T. Kamiyama, O. Terasaki, T. J. Pinnavaia and Y. Liu, *J. Am. Chem. Soc.*, 2003, **125**, 821.
- 19 P. P. Chu and H. D. Wu, *Polymer*, 2000, **41**, 101.
- 20 H. Kosonen, J. Ruokolainen, M. Torkkeli, R. Serimaa, P. Nyholm and O. Ikkala, *Macromol. Chem. Phys.*, 2002, **203**, 388.